03

Laminar-turbulent transition in a smooth channel with local swirling of flow

© V.M. Molochnikov, N.D. Pashkova, A.A. Paereliy

Federal Research Center „Kazan Scientific Center of Russian Academy of Sciences“, Kazan, Russia
E-mail: vmolochnikov@mail.ru

Received February 27, 2025
Revised May 16, 2025
Accepted May 16, 2025

A weakly swirling flow behind a vane swirler in a smooth pipe was investigated experimentally at the Reynolds numbers of the axial flow Re = 240−1640. The swirl ratio variation along the pipe depending on the Reynolds number was analyzed. The following signs of local laminar-turbulent transition were observed in the vicinity of the pipe axis and near the pipe wall: steep rise in the root-mean-square fluctuations of velocity with the increase in the Reynolds number and intermittency occurring in oscillograms of velocity. The mechanism of local turbulization of flow near the wall of the pipe was described.

Keywords: swirling of flow, vane swirler, laminar-turbulent transition, flow intermittency, intensity of velocity fluctuations, Reynolds number.

DOI: 10.61011/TPL.2025.08.61541.20299

Swirling flows are found in various technical applications: heat exchangers, combustion chambers of jet engines, separation devices, etc. Swirling allows for enhancement of heat and mass transfer processes. Most studies of swirling flows have been focused on turbulent flow regimes. However, the interest in laminar swirling flows, which is associated, in particular, with the growing need for microchannel heat exchangers, has been on the rise lately. Vane swirlers are often used to induce local swirling; downstream of these devices, the degree of flow swirling decreases. This issue has been investigated theoretically and experimentally in [1–5]. Analytical expressions characterizing the reduction in the degree of flow swirling have been obtained, and the process has been modeled numerically [3]. Several studies of laminar swirling flows focused on the stability of a vortex forming downstream of a swirler, which is an issue common to laminar and turbulent flow regimes, have already been published [6]. In the case of laminar flows, the main focus of such studies is on the process of destruction of the precessing vortex core [7–10]. The issues of a laminar-turbulent transition of a swirling flow in a smooth pipe are barely examined.

In the present paper, we report the results of experimental studies into the laminar-turbulent transition in a smooth straight pipe with internal diameter $d = 17.4$ mm after local flow swirling induced by a swirler with four vanes. The length of the swirler along the channel axis is $2d$. The angle of vanes is 0° at 4 mm ($0.23d$) from the swirler inlet and then goes to 23° with a rounding of 6 mm. The vanes make 0.23 turns within the swirler length. Their thickness is 1 mm, and the degree of flow blockage by the vanes is 14%. The leading and trailing edges of the vanes are rounded by elliptic curves with a major semi-axis of 2 and 3 mm, respectively. There is no center body.

A straight smooth pipe section upstream of the swirler provided a developed laminar flow with a velocity profile matching the theoretical Poiseuille profile.

A specialized setup was used for experiments [11]. The flow of fluid through the test section was driven by a hydrostatic pressure force, which was produced by a head tank with a constant level, and was regulated by a dispenser with a nozzle system. An aqueous solution of glycerol with a mass percentage content of 56.3% was used as the working fluid. The temperature of the working fluid and its kinematic viscosity were checked prior to each experiment. Instantaneous velocity vector fields were measured using the smoke image velocimetry (SIV) technique [12] in the diametral plane of the pipe and in planes parallel to it, which provided an opportunity to obtain data on the longitudinal and circumferential components of the flow velocity. The fundamental difference between SIV and the traditional PIV method is the significantly higher concentration of tracers that does not yet affect the flow. Instead of tracking the motion of individual tracer particles, the image processing algorithm tracks fragments with the same brightness distribution. SIV provides a higher spatial resolution and lower noise levels than the traditional PIV method.

Measurements were performed at Reynolds numbers $\mathrm{Re} = \langle U \rangle d/\nu = 240$, 500, 800, 1200, 1500, and 1640. Here, ν — kinematic viscosity of the working fluid and $\langle U \rangle$ — average-flow-rate velocity in the pipe. The largest uncertainty of the velocity measurement results in the present experiments varied from 1.8% at Re = 240 to 4.2% at Re = 1640.

Since the ultimate definition of turbulence accounting for all its characteristics has not been formulated yet [13], we will analyze the potential laminar-turbulent transition based on the presence of certain signs of turbulence. In transient

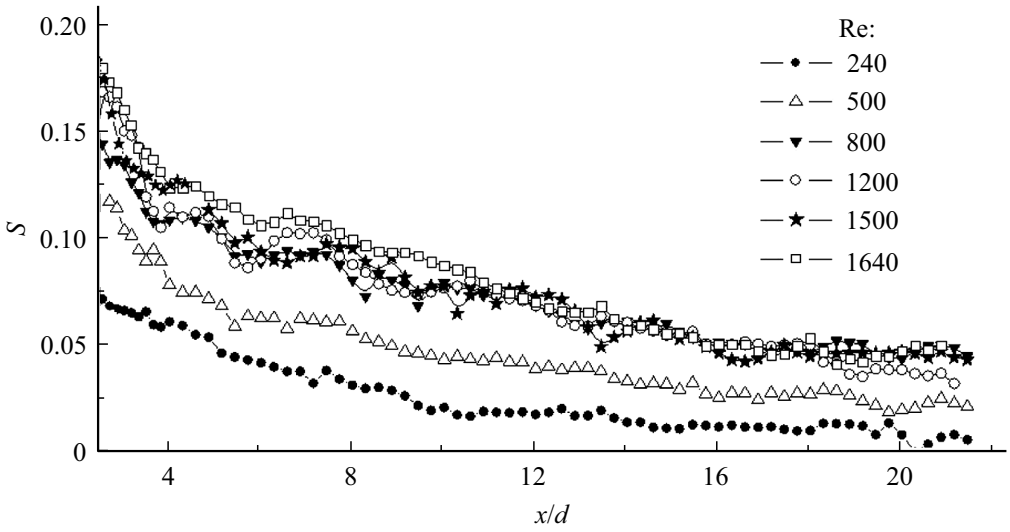

Figure 1. Variation of the degree of flow swirling downstream of a swirler at several different Reynolds numbers.

flow regimes, these signs are a drastic enhancement of root-mean-square fluctuations of the flow velocity in certain regions of the flow with an increase in Reynolds number [14,15] and the emergence of intermittency (alternation of periods of existence of laminar and turbulent flow regimes in the oscilloscope records of flow velocity) [16,17].

The swirler used in the present study produces a weakly swirling flow. Swirling degree

$$S = \frac{\int_0^R \rho U_x U_\theta r^2 dr}{R \int_0^R \rho U_x^2 r dr}$$

was estimated as the ratio of the axial moment of momentum to the total axial momentum. Here, U_θ and U_x are the local circumferential and axial velocities, respectively; r is the current radius; ρ is the working fluid density; and R is the channel radius. Depending on the Reynolds number, the degree of swirling varied within the interval of $0.18-0.07$ at the start of the main measurement area ($x/d = 3-21.5$) and decreased monotonically afterward (Fig. 1).

The measurement method used in the experiments is planar (i.e., confined to a single plane) and does not allow one to perform measurements along spatial swirling flow lines. However, estimates have demonstrated that the maximum value of the circumferential velocity component does not exceed 30 % of the average-flow-rate velocity at the start of the measurement area and decreases with distance from the swirler. Therefore, we consider it possible to analyze the processes of laminar-turbulent transition by examining the behavior of the longitudinal flow velocity component only.

Figure 2, *a* presents the variation of root-mean-square fluctuations $U_{x\,rms}$ on the pipe axis with distance from the swirler at several different Reynolds numbers. It can be seen that the level of fluctuations at $\mathrm{Re} \leqslant 800$ remains virtually unchanged throughout the length of the pipe and is lower than 2.5 % of the average-flow-rate velocity, which is indicative of laminar flow nature. With $\mathrm{Re} = 1200$, $\mathrm{Re} = 1500$, and $\mathrm{Re} = 1640$, fluctuations start to intensify at $x/d \approx 17$, $x/d \approx 13$, and $x/d \approx 10$, respectively. The local fluctuation maxima are 5, 7.5, and 11 %, respectively, and exceed the maximum observed in the turbulent regime (3.2 %). The same fluctuation behavior in the process of laminar-turbulent transition in pipes was reported in [18]. Flow intermittency was observed in the oscilloscope records of the longitudinal flow velocity component in these regions in the indicated regimes. An example oscilloscope record of this kind for $\mathrm{Re} = 1500$, $x/d = 15$ (i.e., in the region of $U_{x\,rms}$ growth) is presented in Fig. 2, *b*. No intermittency was found in the oscilloscope records of velocity at $\mathrm{Re} < 1200$. The obtained results indicate the occurrence of a laminar-turbulent transition in the central part of the channel, which starts at a distance of $x/d \approx 17$ at $\mathrm{Re} \geqslant 1200$ and shifts toward the swirler with increasing Reynolds number.

The results of flow visualization, the lack of a stagnation point and a reverse flow zone in the velocity profiles, and the shape of the oscilloscope record of the transverse velocity component (inset in Fig. 2, *a*) suggest that the vortex formed downstream of the swirler is not destroyed in the examined regimes.

The pattern of variation of root-mean-square fluctuations of the longitudinal flow velocity component near the pipe walls is more complex. An example $U_{x\,rms}(x/d)$ distribution at $r/R = -0.7$ (i.e., at a distance of $0.15d$ from the channel wall) is shown in Fig. 3, *a*. A noticeable local $U_{x\,rms}$ increase with increasing Reynolds number is initiated at $\mathrm{Re} \geqslant 1500$ and is observed in three regions: $x/d \approx 6.9$, 12.0, and 17.6; notably, the first of them is much closer to the swirler than the region of $U_{x\,rms}$ growth on the pipe axis. Note that there are no pronounced local maxima in the $U_{x\,rms}(x/d)$

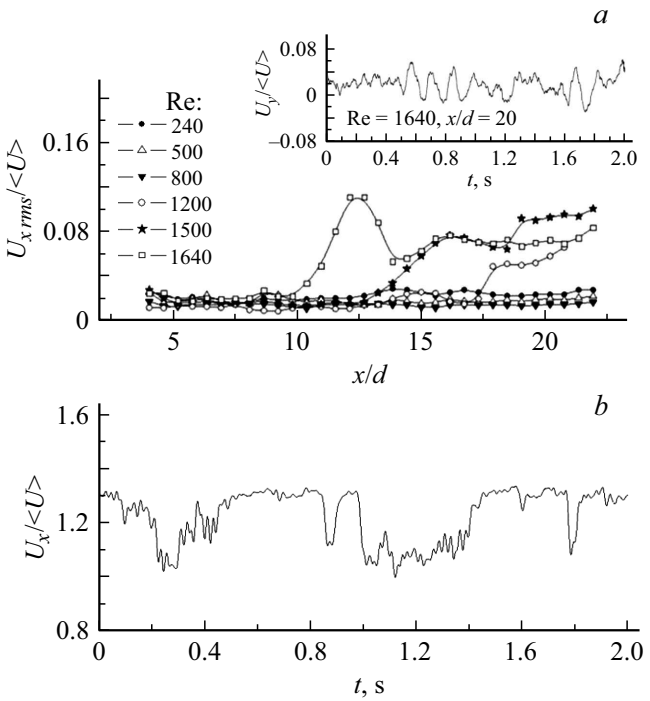

Figure 2. Variation of flow parameters on the pipe axis downstream of the swirler. *a* — Root-mean-square fluctuations of the longitudinal velocity component and oscilloscope record of the transverse velocity at Re = 1640, $x/d = 20$ (inset); *b* — oscilloscope record of the longitudinal flow velocity component at Re = 1500, $x/d = 15$.

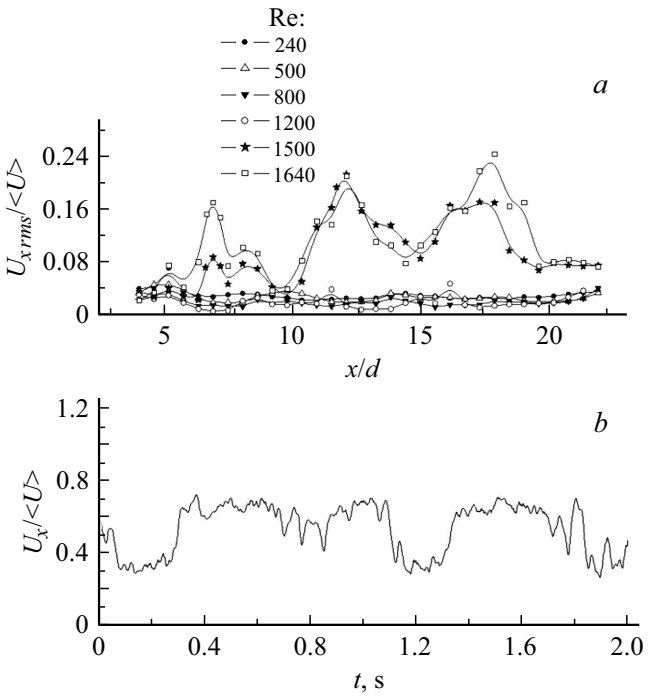

Figure 3. Distributions of the intensity of fluctuations of the longitudinal flow velocity component at $y/R = 0.7$ (*a*) and oscilloscope record of the longitudinal velocity component at Re = 1500, $x/d = 15.5$, and $y/R = 0.7$ (*b*).

distribution at Re < 1200, but the overall fluctuation level is approximately 2.5–4 % (i. e., is somewhat higher than the one on the pipe axis). At Re = 1200, the trend toward the formation of local maxima is evident at $x/d = 11.5$ and 16, but the value of $U_{x\,rms}$ does not exceed 5 % in these regions.

Apparently, the mechanism of periodic local flow turbulization near the pipe wall is as follows. The swirler vanes in the actual experiment have a nonzero thickness. Therefore, regions of velocity defect [19] and wakes are formed downstream of them and move in a spiral away from the swirler. These wakes interact periodically with the pipe wall, causing an increase in intensity of velocity fluctuations and the emergence of local maxima of the $U_{x\,rms}(x/d)$ distributions. The maximum magnitude of root-mean-square velocity fluctuations in these regions is 25 %, which is significantly higher than the level of turbulent fluctuations in the region of developed turbulent flow in a smooth pipe without flow swirling. The distance between $U_{x\,rms}$ maxima varies along the measurement region from $5.1d$ to $5.6d$, which is consistent with the pitch of spiral motion of the wake behind the vanes (with account for the reduction in flow swirl angle with distance from the swirler). At Re $\leqslant$ 1200, the vane wakes appear to be largely blurred by viscous effects, and there is virtually no evidence of a laminar-turbulent transition in the near-wall region within this range of Reynolds numbers.

The occurrence of a local laminar-turbulent transition near the wall at Re $\geqslant$ 1500 is also confirmed by flow intermittency, which is visible in the oscilloscope records of the longitudinal flow velocity component near the wall. An example oscilloscope record of this kind for Re = 1500 at $y/R = 0.7$ and $x/d = 15.5$ is presented in Fig. 3, *b*.

Thus, it was established that signs of a laminar-turbulent transition (an increase in intensity of velocity fluctuations and flow intermittency) may be observed at certain Reynolds numbers (degrees of swirling) in the studied regimes of weakly swirling flow in a smooth pipe. The velocity fluctuations on the pipe axis start to intensify at Re = 1200, and the first local regions of enhancement of velocity fluctuations in the near-wall region are located significantly closer to the swirler. The physical mechanisms of initiation of flow turbulization were detailed. The obtained data may help predict flow parameters in pipes with local flow swirling at low Reynolds numbers. In addition, the results may be used in modeling of natural physiological flow swirling in elements of the human cardiovascular system (specifically, modeling performed in order to choose the parameters of test sections of experimental setups).

Conflict of interest

The authors declare that they have no conflict of interest.

References

[1] L. Talbot, J. Appl. Mech., **21** (1), 1 (1954). DOI: 10.1115/1.4010810

[2] M. Kiya, S. Fukusako, M. Arie, Bull. JSME, **14** (73), 659 (1971). DOI: 10.1299/jsme1958.14.659

[3] T.F. Ayinde, Sadhana, **35**, 129 (2010). DOI: 10.1007/s12046-010-0018-9

[4] S. Yao, T. Fang, Commun. Nonlinear Sci. Numer. Simul., **17** (8), 3235 (2012). DOI: 10.1016/j.cnsns.2011.11.038

[5] F. Beaubert, H. Pálson, S. Lalot, I. Choquet, H. Bauduin, Appl. Math. Mod., **40**, 6218 (2016). DOI: 10.1016/j.apm.2016.02.002

[6] S.V. Alekseenko, P.A. Kuibin, V.L. Okulov, *Vvedenie v teoriyu kontsentrirovannykh vikhrei* (Inst. Teplofiz. Sib. Otd. Ross. Akad. Nauk, Novosibirsk, 2003), p. 420 (in Russian).

[7] M. Escudier, Prog. Aerosp. Sci., **25** (2), 189 (1988). DOI: 10.1016/0376-0421(88)90007-3

[8] A. Bottaro, I.L. Ryhming, M.B. Wehrli, F.S. Rys, P. Rys, Comput. Meth. Appl. Mech. Eng., **89** (1-3), 41 (1991). DOI: 10.1016/0045-7825(91)90036-6

[9] D.J.C. Dennis, C. Seraudie, R.J. Poole, Phys. Fluids, **26** (5), 053602 (2014). DOI: 10.1063/1.4875486

[10] Z. Seifi, M. Raisee, M.J. Cervantes, J. Phys.: Conf. Ser., **2707** (1), 012129 (2024). DOI: 10.1088/1742-6596/2707/1/012129

[11] V.M. Molochnikov, N.I. Mikheev, A.N. Mikheev, A.A. Paereliy, O.A. Dushina, Int. J. Heat Fluid Flow, **96**, 108984 (2022). DOI: 10.1016/j.ijheatfluidflow.2022.108984

[12] N.I. Mikheev, N.S. Dushin, Instrum. Exp. Tech., **59** (6), 882 (2016). DOI: 10.1134/S0020441216060063

[13] S. Ferrari, R. Rossi, A. Di Bernardino, Energies, **15** (20), 7580 (2022). DOI: 10.3390/en15207580

[14] F. Durst, B. Unsal, J. Fluid Mech., **560**, 449 (2006). DOI: 10.1017/S0022112006000528

[15] V.V. Lemanov, V.V. Lukashov, K.A. Sharov, Tech. Phys. Lett., **50** (2), 17 (2024). DOI: 10.61011/PJTF.2024.03.57039.19725.

[16] V. Uruba, *Turbulence handbook for experimental fluid mechanics professionals* (Dantec Dynamic, Skovlunde, 2012), p. 23.

[17] H. Schlichting, *Boundary-Layer Theory* (McGraw-Hill, 1979).

[18] F. Durst, M. Fischer, J. Jovanovic, H. Kikura, J. Fluids Eng., **120**, 496 (1998). DOI: 10.1115/1.2820690

[19] Á. Helgadóttir, S. Lalot, F. Beaubert, H. Pálsson, Appl. Sci., **8** (10), 1865 (2018). DOI: 10.3390/app8101865

Translated by D.Safin